



## EYE LIGHT FLASHES ON THE MIR SPACE STATION

S. AVDEEV

Russian Space Corporation “Energia” Korolev, Korolev, Moscow, Russia

V. BIDOLI, M. CASOLINO, E. DE GRANDIS, G. FURANO, A. MORSELLI,  
L. NARICI, M.P. DE PASCALE, P. PICOZZA, E. REALI and R. SPARVOLI

Department of Physics, University of Rome “Tor Vergata”, INFN, Sez. Rome 2, Italy

M. BOEZIO and P. CARLSON

Royal Institute of Technology, Stockholm, Sweden

W. BONVICINI, A. VACCHI AND N. ZAMPA

Department of Physics, University of Trieste and INFN, Italy

G. CASTELLINI

IROE of CNR, Florence, Italy

C. FUGLESANG<sup>†, ‡</sup>

European Astronaut Centre, ESA, Cologne, Germany

A. GALPER, A. KHODAROVICH, YU. OZEROV<sup>✕</sup>, A. POPOV and N. VAVILOV

Moscow State Engineering Physics Institute, Moscow, Russia

G. MAZZENGA and M. RICCI

L.N.F.-INFN, Frascati, Rome, Italy

W.G. SANNITA

DISM, University of Genova, Genova, Italy

Department of Psychiatry, SUNY, Stony Brook, NY, USA

and

P. SPILLANTINI

Department of Physics of Univ. and Sez. INFN, Florence, Italy

(Received 2 May 2001)

**Abstract**—The phenomenon of light flashes (LF) in eyes for people in space has been investigated onboard Mir. Data on particles hitting the eye have been collected with the SilEye detectors, and correlated with human observations. It is found that a nucleus in the radiation environment of Mir has roughly a 1% probability to cause an LF, whereas the proton probability is almost three orders of magnitude less. As a function of LET, the LF probability increases above 10 keV/μm, reaching about 5% at around 50 keV/μm. © 2002 Elsevier Science Ltd. All rights reserved

<sup>†</sup>Corresponding author. Mail Code OT, NASA Johnson Space Center, Houston, TX 77058, USA. Tel.: +1-281-244-7769; fax: +1-281-7822.

E-mail address: christer.fuglesang1@jsc.nasa.gov (C. Fuglesang).

<sup>‡</sup>Also visiting Royal Institute of Technology.

<sup>✕</sup> Deceased.

## 1. INTRODUCTION

Unexpected visual sensations during space flights were first reported after the Apollo-11 flight to the moon in 1969 [1]. These phenomena, which became known as light flashes (LF), were subsequently also reported by astronauts on Apollo-12 and Apollo-13. They appeared as faint spots or flashes of light after some dark adaptation and occurred spontaneously and randomly. It is interesting to note that already in 1952, it had been hypothesized that people outside the shielding provided by Earth's magnetic field were likely to see flashes of light from cosmic particles [2]. During the remaining Apollo flights, a total of 12 astronauts carried out about 20 h of LF observations. It was found that on average, after about 15–20 min of dark adaptation, about one LF per 3 min was seen [1]. Three basic types of flashes were reported at the time: “spots” or “star-like” flashes, “streaks” and “clouds”.

At the same time, several studies were performed with accelerator beams, exposing the human eye and brain to well-defined particle fluxes. It was found that neutrons, with energy of more than about 5 MeV, could cause LF sensations [3–6], but a beam of  $\pi^+$  mesons with momentum 1.5 GeV/ $c$  did not create any effect [5]. Studies using muons (cosmic [7,8] and a 6 GeV/ $c$  beam [9]) also reported LF effects. During dedicated observations in high-altitude (9–16 km) aircrafts LFs were seen, but they were considered to be partly of a different nature than those in space, possibly due to a different particle composition in the radiation environment [10].

Several possible explanations were put forward to explain this phenomenon. They included Cherenkov light in the vitreous [11], a direct excitation of the retina by ionization [11,1], an indirect effect from protons knocked out by neutrons [3] or from alpha-particles from reactions with C, O or N atoms [6]. It was also suggested that scintillation in the eye lens could cause the observed LFs [12]. Experiments with helium and nitrogen beams, however, seemed to pinpoint the effect to the retina as well as indicating that the dominating effect is due to local energy deposition, possibly in the outer segments of rods and cones since dark adaptation is necessary to observe LFs [13,14]. It is also worth noting that these experiments did not note any light sensations when beams passed through the optical nerve or the visual cortex of the brain.

Still many questions remained to be answered. Among them is the question as to which particles in space cause the LFs in astronauts and their fre-

quency in Earth orbits. Furthermore, it was not completely ruled out that the Cherenkov effect, or some other effect could play a role during space flights. Therefore, experiments were performed on Skylab in 1974 [15] and on Apollo during the Apollo–Soyuz project in 1975 [16]. Correlation with particle fluxes was done, suggesting a relation with ions having linear energy transfer (LET) greater than 5 keV/ $\mu\text{m}$  in tissue [16]. However, no conclusive results were obtained and some results even seem contradictory. For instance, on Skylab a big increase in the LF rate was seen in the South Atlantic Anomaly (SAA), whereas in Apollo no such increase was observed. A recent discussion on the biological aspects of LFs can be found in Ref. [10].

The aim of the SilEye (from Silicon Eye) project, presented here, is to conduct a systematic study of the LF phenomenon over several space missions and subjects (astronauts). Two active particle detectors have been built, based on silicon technology, and sent to the Russian Mir space station. A real-time particle-tracking detector was placed close to the subject's eye and detector data as well as the subject's reaction to LFs were recorded on computer disks. Between 1995 and 1999, in total, 10 astronauts participated in the SilEye project, but two of them reported not seeing light flashes at all and two others only saw two flashes each during several sessions. During the Apollo flights, there was also one subject who did not notice any LFs, although briefed about it in advance [1]. The SilEye computer disks with data were brought back to Earth for analysis. In this way, particles passing through the eye could be identified and correlated in time with LFs. It should be mentioned that during Apollo-16 and Apollo-17, an emulsion experiment (ALFMED) made a similar attempt and two events were found coinciding with LFs [1].

The SilEye project is a part of the Russian — Italian mission (RIM) program [17] which conducts a general study of cosmic rays using space-borne apparatuses equipped with silicon particle-tracking detectors. The other projects are the experiments Nina [18] and Nina2 [19] on the “Resurs01” No. 4 and MITA0 satellites, respectively, and the planned Pamela detector [20] for a future satellite. The SilEye project has built and sent two apparatuses, SilEye-1 and SilEye-2 to Mir.

This paper presents results from the LF observations on Mir with the SilEye apparatuses between 1995 and 1999. It is the most extensive study of the LF phenomenon in space ever. In particular, we wanted to investigate the hypothesis that heavy ions are the dominant source for LFs. For the first

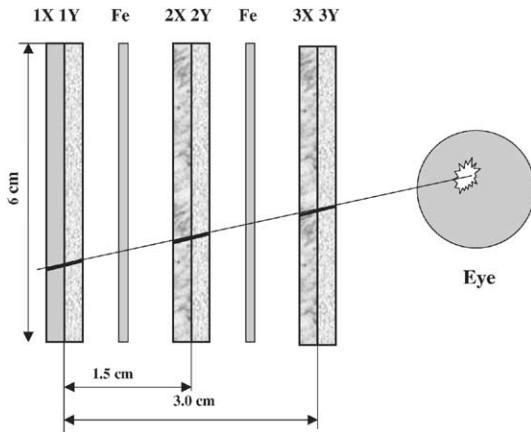


Fig. 1. A schematic view of the SilEye-2 detector. The three planes of double silicon layers are interleaved with two 1-mm iron absorbers. A particle track hitting the eye is shown.

time, active detectors that can track particles and correlate them with LFs have been used in space for this task. In this work, we present the data from the second detector (SilEye-2), the analysis of tracks and particles will only use these data. Section 2 gives an explanation of the SilEye experiment and a brief overview of the Mir space station. In Section 3, data collection and analysis are described and in Section 4 the main results and discussions are reported. Conclusions are given in Section 5.

## 2. SILEYE APPARATUSES AND MIR SPACE STATION

The SilEye detectors are derived from technology developed for the Nina cosmic ray space apparatus [18]. The basic part is made of two  $60 \text{ mm} \times 60 \text{ mm} \times 0.38 \text{ mm}$  semi-conducting silicon layers, each divided into 16 strips  $3.6 \text{ mm}$  wide, perpendicularly oriented to give an  $x$ - $y$  reading plane. Three such planes constitute the whole detector. For SilEye-2, the distance between the planes is  $15 \text{ mm}$ , interleaved by two  $1 \text{ mm}$  iron absorbers to increase particles' energy loss between planes in order to increase the particle identification power (Fig. 1).

The energy loss by particles traversing the silicon planes is measured with the amplifier system sensitive from a loss of  $0.25 \text{ MeV}$  to a maximum of  $260 \text{ MeV}$  (corresponding to  $12 \text{ pC}$ ). The analog preamplifiers are mounted on the sides of the silicon planes. The read-out of the strips is triggered by a coincidence of the 16 strips summed signals between the planes 1 and 3. If the signal of both planes is more than a value corresponding to

$2.5 \text{ MIP}^\dagger$  a trigger signal is given. For SilEye-2, a trigger threshold of  $2.5 \text{ MIP}$  was chosen to exclude high-energy protons, which had saturated the SilEye-1 detector in the SAA. Roughly, the high-energy cut-off value for protons is  $200 \text{ MeV}$ , but there is no cut-off for particles with charge  $Z \geq 2$ . The integration time of the signal is about  $2 \mu\text{s}$ .

A 12-bit ADC converts the analog signal and the digitized information is transmitted via a parallel interface to an IBM ThinkPad 750C laptop computer (provided by ESA), and stored on PCMCIA cards. To save storage volume, a pedestal subtraction is done and only strips with a signal larger than three standard deviations above noise level are saved. Strip numbers, strip signal amplitudes and time are written for each event. Maximum readout rate is  $100 \text{ Hz}$ .

A prototype detector for SilEye-2, without Fe absorbers, was tested and calibrated with proton beams of  $48$  and  $70 \text{ MeV}$  at The Svedberg Laboratory (TSL), Uppsala, Sweden, showing good linearity of the device and an energy resolution of  $4$ – $6\%$  [21]. The detector to fly was subsequently calibrated both at TSL and at GSI (Darmstadt, Germany) with beams of  $\text{C}^{12+}$ . An identical copy of the flight detector has also been calibrated in Uppsala and is used for crew training and verification on ground, if necessary.

The silicon detector is encased in an aluminum box and mounted on a kind of helmet worn by the astronaut (Fig. 2). The detector is positioned on the side of the subject's right eye, close to the temple. In front of the eyes, there is a mask with three light-emitting diodes (LEDs). Two LEDs are used to position the helmet properly in relation to the eyes, and the third diode is for checking the subject's dark adaptation and reaction time. The astronaut holds a joystick with a button that is pressed when he (so far all subjects have been men) sees a light flash. The joystick is connected to the detector electronics and the recorded times of button pressings are sent to the computer and written to the PCMCIA card.

The SilEye-1 apparatus was sent to the Russian Mir space station in October 1995 and was used through 1996. Several important improvements, including better electronics and adding some LEDs to test for dark adaptation and reaction time, were introduced in SilEye-2. This apparatus was built in 1997 and sent to Mir late the same year. Mir

<sup>†</sup>MIP (minimum ionizing particle) is a relative measure of ionization. One MIP is the signal given by a high-energy singly charged particle ( $\geq 1 \text{ GeV}$  for a proton).

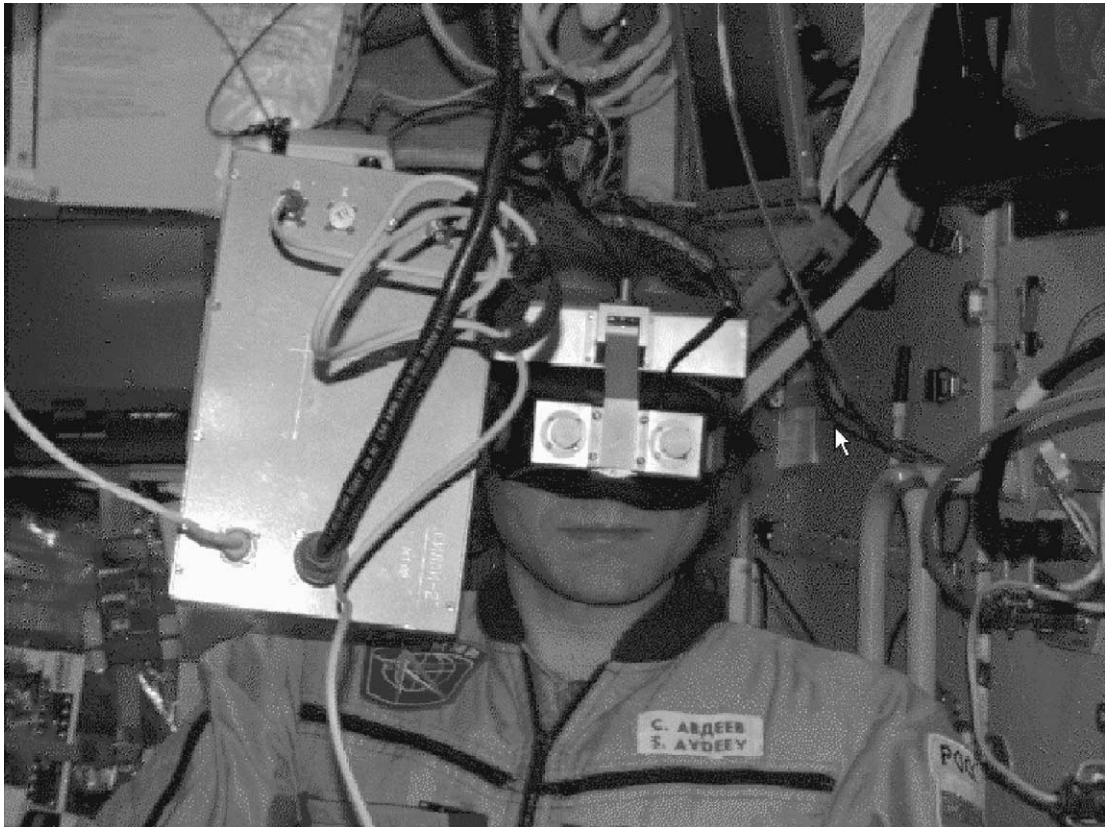


Fig. 2. An astronaut on Mir with the SilEye-2 detector mounted on the side of his head and the mask with LEDs in front of his eyes.

(“World” or “Peace” in Russian) itself has been in space since February 1986, when the core module was launched. Over time, five more modules have been added, the last being Priroda (“Nature” in Russian) in 1996 (Fig. 3). The modules are more or less cylindrically formed, with diameters of 3–4 m and lengths of 13 m and a mass of 20 ton (except the Kvant module, which is about half as long and heavy). In addition, normally one Soyuz crew vehicle and a Progress transport vehicle are docked to the station. They are each about 7 m long, 2–3 m wide and have a mass of 7 tons. In 1995/96, the LF observation sessions were done in the crew cabins of the core module, while the sessions with SilEye-2 in 1998/99 took place in the modules Kristall and Priroda. There is a considerable amount of passive material of the spacecraft surrounding the subject, in which primary cosmic particles can interact and produce showers of secondaries. The amount of material varies from place to place and according to the trajectory of the particles.

Mir is orbiting at altitudes around 350–400 km with an inclination of 51.6 deg. From November 1995 to January 1996, the LFs were detected at altitudes between 400 and 415 km. During the first

observations in August 1998, the station altitude was around 400 km but slowly decreased to 355–360 km for the last sessions in June 1999.

### 3. DATA COLLECTION AND ANALYSIS

The data used for this paper were collected during two periods. The first was from 24/11/95 to 19/1/96 involving the three astronauts (subjects) of Mir expedition-20 and the second period was from 18/8/98 to 29/6/99 during expedition-26 and expedition-27. Four astronauts participated in the second period, one of them also flew on expedition-20. In the 1995/96 period, a total of 87 LFs was noted during nine sessions, with a total observation time of 492 min. In the second period 1998/99, we have 17 sessions with simultaneous SilEye-2 detector and LF observation data. During about 800 min of observation 116 LFs were seen. An additional 30 LFs were noted during three observation sessions amounting to 250 min without silicon detector. Overall, the average time between LFs was about 7 min. For particle and radiation studies, the SilEye-2 apparatus has also taken large amounts of data in an autonomous mode, close to

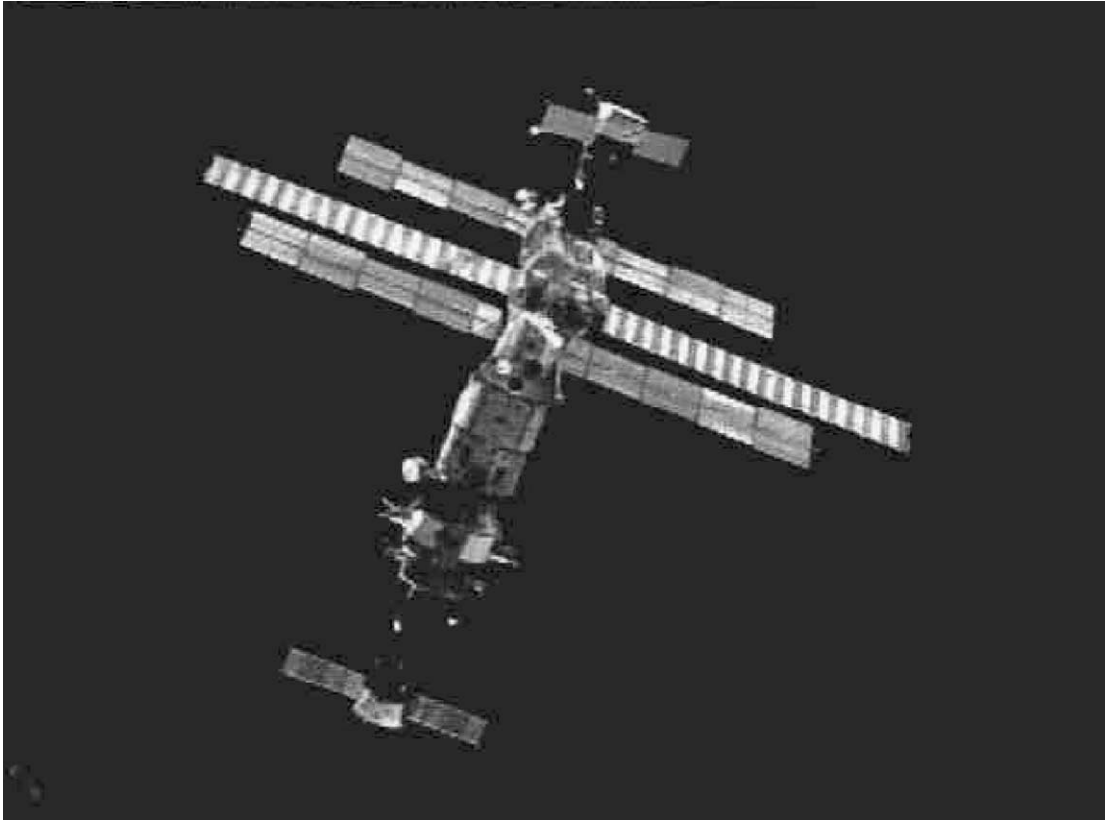


Fig. 3. Mir space station.

1000 h of registration. Analysis of these data is in progress and will be published later. However, some preliminary results can be found in Ref. [22].

Each observation session begins with 15 min of dark adaptation, checked in SilEye-2 with LED pulses. The LED flashed every minute, starting with a very short pulse of 8  $\mu$ s. If there is no reaction from the subject, i.e. the joystick button is not pressed, then after 2 s there is a new pulse, twice as long. The light pulse is doubled every 2 s until the button is pressed by the subject noting the light. The reaction time and final pulse length are recorded by the computer. It was found that already after 5 min the subject's sensitivity did not increase significantly more, typically staying around 2 or 4 ms pulses, but with some fluctuations as well as variations between subjects. The same was found during ground data collection, but with less fluctuations after the high sensitivity limit was reached.

At the start and end of each data collection session, the detector performs a self-calibration. Noise level, pedestal position and detector linearity are checked and calibration coefficients are calculated. No drift over time was noted and, indeed, the detector noise turned out to be lower on Mir than on the ground.

Table 1. Data summary

Event type	Number	Average frequency (Hz)
Triggers	241,742	$4.95 \pm 0.01$
Tracks	116,366	$2.38 \pm 0.01$
Protons	115,508	$2.36 \pm 0.01$
Nuclei	858	$0.018 \pm 0.001$
Showers	4434	$0.908 \pm 0.014$

*Note.* The frequency is a total average and shows a considerable variation with location.

After each observation session, the subject writes comments on the PCMCIA card. The comments are typically on the nature of flashes seen or if something particular happened. Thus for each observation session, we obtain three files: detector data on particle tracks, LF-times and astronaut comments.

The detector automatically starts to record particle data at the end of the 15 min dark adaptation. In total, during 17 sessions the detector registered 116,366 clean events, which were recorded in 48,850 s. This corresponds to an average trigger rate of 4.9 Hz. About half of the events could be identified as tracks, and we were able to distinguish between protons and nuclei, or a "shower" (see below). Table 1 summarizes the data.

Proton.						
	1X	2X	3X	1Y	2Y	3Y
1	—	—	—	—	—	—
2	—	—	—	—	—	—
3	—	—	—	—	—	—
4	—	—	—	—	—	0.24
5	—	—	—	—	0.20	—
6	0.46	—	—	0.65	—	—
7	—	0.19	—	—	—	—
8	—	—	0.13	—	—	—
9	—	—	—	—	—	—
10	—	—	—	—	—	—
11	—	—	—	—	—	—
12	—	—	—	—	—	—
13	—	—	—	—	—	—
14	—	—	—	—	—	—
15	—	—	—	—	—	—
16	—	—	—	—	—	—

Nucleus						
	1X	2X	3X	1Y	2Y	3Y
1	—	—	—	—	—	—
2	—	—	—	—	—	0.06
3	0.29	—	—	—	—	—
4	—	—	—	—	—	0.62
5	0.16	—	—	—	—	0.60
6	—	—	—	—	0.57	—
7	0.10	0.11	—	—	—	—
8	1.57	—	0.20	—	0.17	0.36
9	101.61	4.21	0.84	0.34	0.50	0.41
10	4.43	6.48	0.77	0.04	0.52	3.81
11	1.63	112.13	2.88	—	1.96	96.47
12	—	2.91	100.17	0.89	101.99	3.21
13	0.09	1.61	5.53	3.50	8.55	—
14	1.95	—	1.24	102.34	0.32	0.33
15	—	—	—	3.70	0.71	—
16	—	—	—	—	—	—

Shower						
	1X	2X	3X	1Y	2Y	3Y
1	—	—	—	—	—	—
2	—	—	—	—	—	—
3	—	—	—	—	—	—
4	—	—	—	—	0.10	0.70
5	—	—	—	0.07	0.31	—
6	—	0.44	—	—	0.05	—
7	—	—	1.52	—	—	—
8	0.12	—	0.48	—	—	—
9	—	0.31	—	—	—	—
10	—	1.12	2.53	—	—	—
11	—	0.43	1.78	—	—	—
12	—	0.10	—	—	0.40	1.87
13	0.26	—	2.67	0.21	—	3.68
14	—	—	—	—	0.20	1.02
15	—	—	0.44	—	—	0.81
16	—	—	—	—	—	—

Fig. 4. Examples of proton, nucleus and shower signals. Amplitudes (energy release in MeV; 1 MIP  $\approx$  0.1 MeV) vs strip number in the six layers (see Fig. 1). Note the clear tracks for the proton and the nucleus. The nucleus has a charge  $Z$  about 24.

Tracks are required to have at least one strip hit (signal above noise level) in five out of the six silicon layers. For an ideal track, only one strip is hit in each layer. This is often the case for low-ionizing tracks, presumably fairly high-energy protons, but medium- and high-ionizing tracks (low-energy protons, nuclei) are usually accompanied by many hit strips. Typically, there is one strip in each layer with

a large signal and several strips with a small signal, consistent with one MIP (Fig. 4). To search for tracks, the signal's center of gravity for each layer is calculated. If the three centers fall on a straight line, we have a track. Further, it is checked whether the line passes through the eye. Another class of events is "showers", defined by having at least 20 strips hit (from all layers), but there is no track as

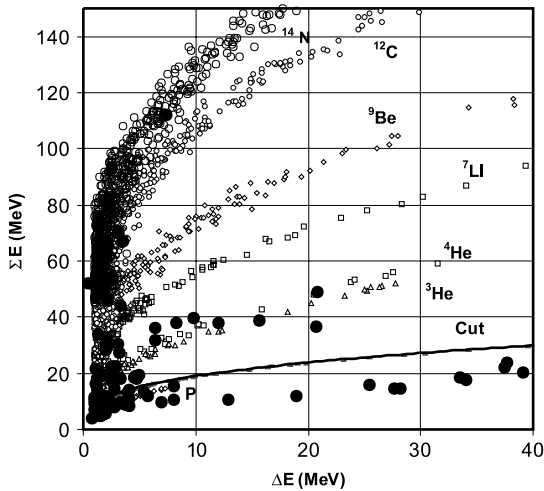


Fig. 5.  $\Sigma E$  vs  $\Delta E$  scatter plot for the SilEye-2 detector simulation. All the smaller points show the simulated values for various nuclei, whereas the larger black circles are real data from one small data sample. The right end of each nuclei scatter, corresponds to the lowest energy for the nucleus to traverse the detector. The continuous line shows the cut used to distinguish between protons and nuclei.

defined above. Presumably, these events are several low-ionizing particles, probably protons, passing through the detector at the same time (within  $2 \mu\text{s}$ ). By inspection, though, one can sometimes see a nucleus track among the other signals. All nuclei and shower events which were candidates for LF were visually inspected.

The signal amplitudes from the strips are proportional to the energy losses in the semi-conductor material, and proportional to the square of the charge of a passing particle ( $Z^2$ ). The energy loss also depends on the energy of the particle, according to the Bethe-Block formula. By combining the amplitude information from the three planes, it is possible to distinguish between various nuclear species in the approximate energy range 40–200 MeV/n, somewhat depending on the nuclear charge. Denote the energy deposited in plane  $i$  as  $E_i$ , the sum of the energies deposited as  $\Sigma E = E_1 + E_2 + E_3$  and the difference between energy deposited in the first and third layers as  $\Delta E = |E_1 - E_3|$ . In a  $\Sigma E$  versus  $\Delta E$  scatter diagram they fall in bands, each band corresponding to a different nucleus (Fig. 5). For fixed  $\Delta E$ ,  $\Sigma E$  increases with the charge. For low-energy particles, the stopping power of the detector is large so that also the difference between the energies deposited in the first and third layers is large. Very low-energy particles, however, will not go through the detector, while at high energies, all events tend

Table 2. Energy ranges for which some nuclei are identified and the energy can be estimated

Nuclei	Charge ( $Z$ )	Energy range (MeV/n)
$^{56}\text{Fe}$	26	161–593
$^{28}\text{Si}$	14	118–386
$^{20}\text{Ne}$	10	97–356
$^{16}\text{O}$	8	85–345
$^{11}\text{B}$	5	62–258
$^7\text{Li}$	3	45–192
$^4\text{He}$	2	39–168
$^1\text{H}$ (proton)	1	38–167

to cluster together at small  $\Delta E$  values with large tails in the  $\Sigma E$  distribution for individual species, thus considerably decreasing the separation power.

Table 2 gives examples of energy ranges for identified nuclei. Note that this method of identifying charge and energy is different from what is normally used, e.g. when the full energy versus  $dE/dx$  is plotted, and, as far as we know, our experiment is the first in which this method has been used in practice.

For higher energies, nuclear discrimination can be obtained for heavier nuclei ( $Z > 4$ ) by requiring a single track and imposing that the energy deposited in the first and third planes differ by less than 20%, and then looking at the total energy loss,  $\Sigma E$ . The distribution of  $\Sigma E$  thus obtained, from our large sample of data of SilEye-2 operating in autonomous mode, is shown in Fig. 6. It is possible to observe how the elemental peaks of the most abundant species up to nickel are easily distinguished, allowing for detailed studies of the radiation environment onboard Mir in conditions of solar quiet and active periods.

In this work, however, we are mostly concerned with the discrimination between protons and heavier particles in order to assess the different contributions to the LF phenomena.

In our analysis presented here, we distinguish between “protons” and “nuclei”, as defined by the cut shown in Fig. 5. The cut is drawn in the middle between the theoretical average proton curve and the curve for  $^3\text{He}$ . We find that of the more than 116,000 tracks, only 858 are clean nuclei (see Table 1), i.e. 0.74% of all tracks. As a comparison, cosmic rays outside the SAA contain 90% protons, 9% He and 1% heavier nuclei. Inside SAA, the proton dominance is much larger.

## 4. RESULTS AND DISCUSSION

### 4.1. Appearance and types of light flashes

A total of 233 LFs reported by six different astronauts is used in the analysis. Four of the astronauts

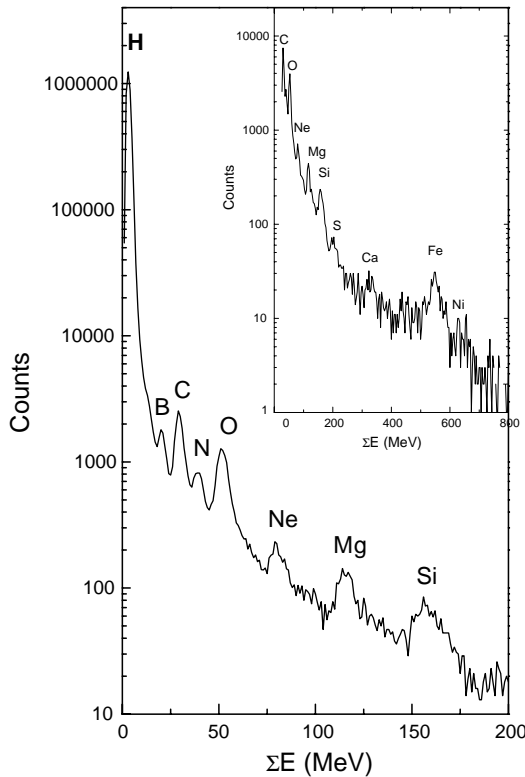


Fig. 6. Nuclear discrimination capabilities of SiEye-2 for high-energy nuclei is shown by this  $\Sigma E$  distribution of data collected in autonomous mode. A cut in the difference of energy deposited in planes 1 and 3 has been imposed (less than 20% difference).

were interviewed after their flights to obtain subjective and more detailed information in addition to the commentary files written after each observation session. They describe five different types of visual sensations:

- a continuous line
- a line with gaps
- a shapeless spot
- a spot with a bright nucleus
- concentric circles.

The first two types make up about 90% of all LFs. This is similar to the Skylab report [15], but different from the Apollo flights (to the moon [1] as well as during Apollo–Soyuz [16]) where “spots” or “star-like” flashes dominated and only about one quarter of the events were described as “streaks”.

All astronauts interviewed reported that in most cases they could confidently indicate a direction of motion of the light (from right to left, from left to right, into the eye, out of the eye). This has also been noted in ground experiments [6,13], but it is difficult to find a physical explanation since particles cross the eye in about 0.1 ns.

#### 4.2. Average time between light flashes and astronauts’ sensitivity

The overall average time between LFs is 6.8 min, but there are differences between individuals as well as possible changes in a specific person’s LF sensitivity over time or between sessions. Of particular interest is one subject, a first-flyer in space, who only after having been instructed by an experienced astronaut could notice LFs. One of the authors (S. Avdeev) who flew on Mir 6 months in 1992/1993, again 6 months in 1995/96 and another 12 months in 1998/99 thought that the frequency of LFs decreased with each subsequent flight. A similar statement was given by a member of Mir expedition-21, who during his first flight (in 1994) had seen frequent LFs but during his entire second flight (in 1996) saw only two LFs (both before sleep). Data from Avdeev’s observation sessions support his feeling: in 1995/96 the average time between his LFs was  $6.2 \pm 1.0$  min while it was  $7.9 \pm 0.8$  min in 1998/99. This could also be an effect of human aging. Table 3 summarizes the observation times, number of LFs and average time  $\tau$  between LFs, for the subjects.

The slight increase in  $\tau$  between the 1995/96 and the 1998/99 sessions is not really significant. However, there is a considerable difference if compared to the results on Skylab in 1974, and to a lesser degree with the Apollo–Soyuz test project (ASTP) in 1975. On ASTP [16] during one orbit, two subjects observed LFs with an average  $\tau$  per subject of 2.2 min. It should be noted, though, that there have been SiEye sessions where  $\tau$  was around 3 min. Two observation sessions took place on Skylab [15], with a total average  $\tau$  of  $0.74 \pm 0.06$  min. What was particularly striking on Skylab is the huge rate observed in the SAA averaging 0.2 min/LF for the two sessions. No SAA increase was observed on Apollo and there is only a slight increase in SiEye SAA data. One could speculate on a dependence of LFs with solar activity and in Fig. 7, we compare  $\tau$  for all data with monthly solar spot number (SSN). There does not seem to be any correlation.

During the dedicated moon-flight studies, it was consistently noted that the average time between LFs was about two times longer when coming back from the moon compared to when going to the moon [1]. A good explanation for this was never found. One possible explanation could be that a person’s LF sensitivity decreases with time in space. The best SiEye data for examining this possibility come from two subjects: The first performed 12 observations between his flight-day 74 and flight-day 320 while the second did five sessions between his flight-day 30 and flight-day 110. No flight-time

Table 3. Observation time, number of LFs and average minutes per LF for the three subjects in the 1995/96 period and for the four subjects of the 1998/99 one. Errors are only statistical. Not included are errors from time estimates and factors due to the fact that different subjects might have different LF sensitivity

	N1- 1995/96	N2- 1995/96	N3- 1995/96	Total 1995/96	N1- 1998/99	N4- 1998/99	N5- 1998/99	N6- 1998/99	Total 1998/99	All
Time (min)	260	171	61	492	642	117	27	301	1087	1579
LF	42	37	8	87	81	32	9	24	146	233
$\tau = \text{min/LF}$	6.2	4.6	8	$5.7 \pm 0.6$	7.9	3.7	3	13	$7.4 \pm 0.6$	$6.8 \pm 0.5$

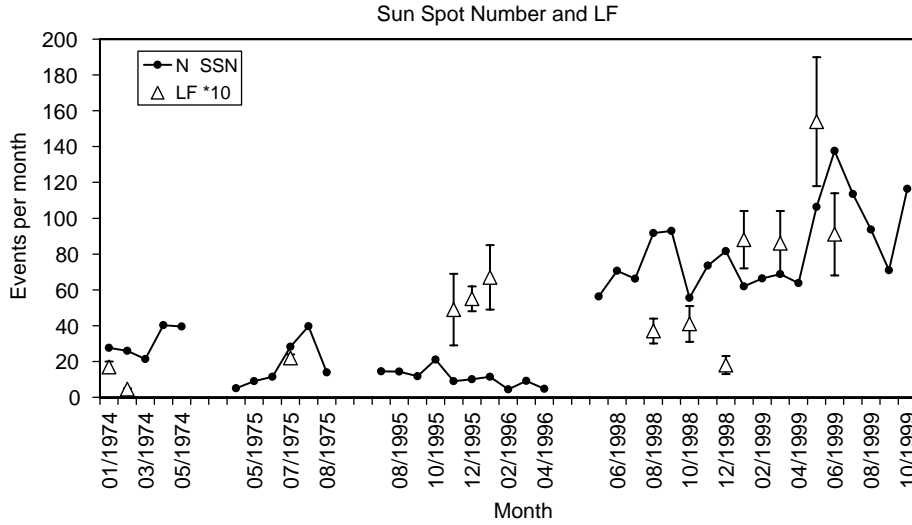


Fig. 7. Average time  $\tau$  between LF in different months compared to the monthly variation of the sun spot number (SSN). Skylab, Apollo–Soyuz and all SiEye data.

dependence at all was found in those data. However, data from a third subject, who made two sessions on his flight-days 5 and 8, show a possible effect. On flight-day 5,  $\tau$  outside SAA is  $3.6 \pm 0.7$  min versus  $8.1 \pm 3.7$  min on day 8, and the corresponding  $\tau$  in SAA are  $1.7 \pm 0.8$  and  $2.0 \pm 0.9$  min, respectively. Unfortunately, we do not have more data from early flight-days, but this should be looked into for more details during future flights. Our results, and the moon-flights data, are fully consistent with the assumption that a person’s LF sensitivity decreases significantly during the first one or two weeks in space, but then remains constant. Considering that many other physiological parameters are modified considerably during the first weeks in space, this is not implausible. At the beginning of each session, the subject was tested for his dark adaptation and light sensitivity, but there is no noticeable difference between the two sessions.

4.3. Geomagnetic dependence

The geographical distribution of all the SiEye LFs is shown in Fig. 8. It must be noted that these data are not normalized to time spent observing in

a certain region, and in particular during 1995/96 most sessions were done during orbits passing through the SAA. An example of such an orbit is shown in the figure.

In Fig. 9, we compare rates of LFs with different types of events (protons, nuclei, showers), including and excluding SAA data, as a function of geomagnetic rigidity. The geomagnetic rigidity  $R$  for a point in the geomagnetic field is defined by the minimum rigidity that a particle coming from infinity must have to reach that point. The rigidity of a particle is given by the quantity  $pc/Ze$ , where  $p$  is the momentum and  $Z$  the charge of the particle. For each LF we have the latitude, longitude and altitude of Mir at that moment and can calculate  $R$  from a model of the geomagnetic field. High latitudes correspond to small  $R$ -values. At the equator  $R$  is around 17 GV and at the SAA has values of 8-12 GV. There is no difference between 1995/96 data and 1998/99 data; therefore, all data have been combined (Fig. 9a).

Figure 9b shows the proton rates, all data and data outside SAA only, obtained by SiEye-2 during the 17 observation sessions in 1998/99. Although the trigger threshold is 2.5 MIP, there is still a large increase of the rate in SAA. SiEye-1 has a trigger

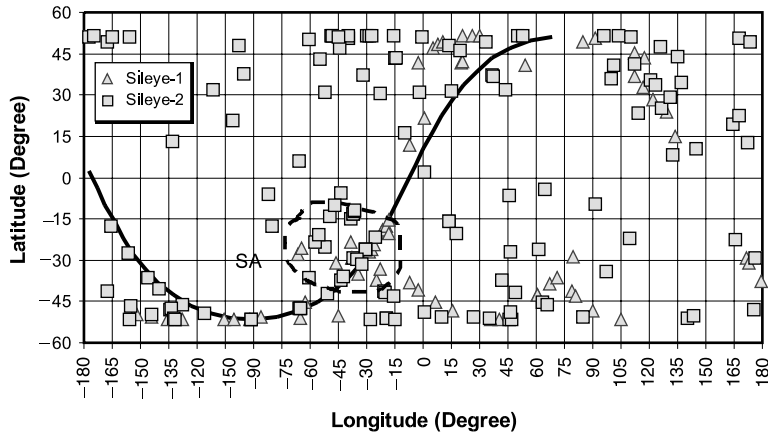


Fig. 8. Geographical distribution of all 233 LFs. An example of a typical measurement session (part of an orbit) going through the SAA is shown by the curve. The indicated area corresponds to the South Atlantic Anomaly (SAA).

threshold of 0.5 MIP, and its trigger rate saturated in SAA at 25 Hz [23,24]. There is a much smaller difference between nuclear spectra ( $Z \geq 2$ ), for all data and for those outside SAA, as seen in Fig. 9c. This is expected, since most trapped particles in the radiation belts are protons. There are some trapped alpha-particles ( $^4\text{He}$ ) in the SAA, which cause the small bump in the all-data nuclei spectra. The shower rate distribution is shown in Fig. 9d. While the proton and nuclear distributions are very similar in shape when excluding SAA, although some 50 times higher for protons, the shower distribution is quite different and we also note that there is no difference inside and outside the SAA. On the other hand, the shower rate drops below some 5 GV rigidity. This shows that showers are caused by high-energy (galactic) protons, with energy above 5 GeV, most likely interacting with material of the space station.

The general trends of the LF-distribution are similar to those of protons and nuclei but, due to the limited statistics of the LF distribution, it is not possible to make direct comparisons with either particle distribution. However, since the rate of LF in SAA is only slightly higher than the rate outside for the same geomagnetic rigidity, we can conclude that high-energy protons cannot be the main reason for LFs. It is to be noted, that the proton rate in SAA is much higher than that measured due to the limited energy ranges of our detectors (40–200 MeV for SilEye-2 and  $> 25$  MeV for SilEye-1).

#### 4.4. Light flashes correlated with particles

In order to search for individual candidate events causing LFs, we look for particles with a track go-

ing through an eye. The detector covers a geometrical solid angle of only some 4% of the two eyes, but since the detector registers particles in any direction, the acceptance is effectively twice this value. On the other hand, there is some loss due to particles stopping in the head between an eye and the detector, so a rough estimate of the overall acceptance is 6–7%. For showers, we make the assumption that there is always at least one particle going through the eye.

Next we look into a reaction time window preceding the recorded LF time. The dark adaptation data give good statistics on each individual's reaction time to stimulus and any possible change over time spent in space. We found that there is no change during the period of the flight and no difference between ground and flight data. All subjects have similar reaction times and therefore we have combined all data, shown in Fig. 10.

From the reaction time distribution, we chose a window between 1.2 and 0.2 s before the joystick signal notifying an LF by the subject. Any particle registered by the detector in that time frame is a candidate for causing the LF. If a particle is outside this time window, then it is excluded. Tables 4–6 summarize the data. The particle rates in the tables have been corrected for the detector dead time of 0.01 s which particularly in the SAA is significant due to the high trigger rate of 24 Hz.

Both proton and nuclei rates increase significantly in the LF windows. The nuclei flux does not differ very much inside and outside SAA, while the proton flux is orders of magnitude larger inside. Although the total time of SAA data is 5768 s or 12% of all data time, 70% of the protons are there. The SilEye-2 detector only triggers on protons with

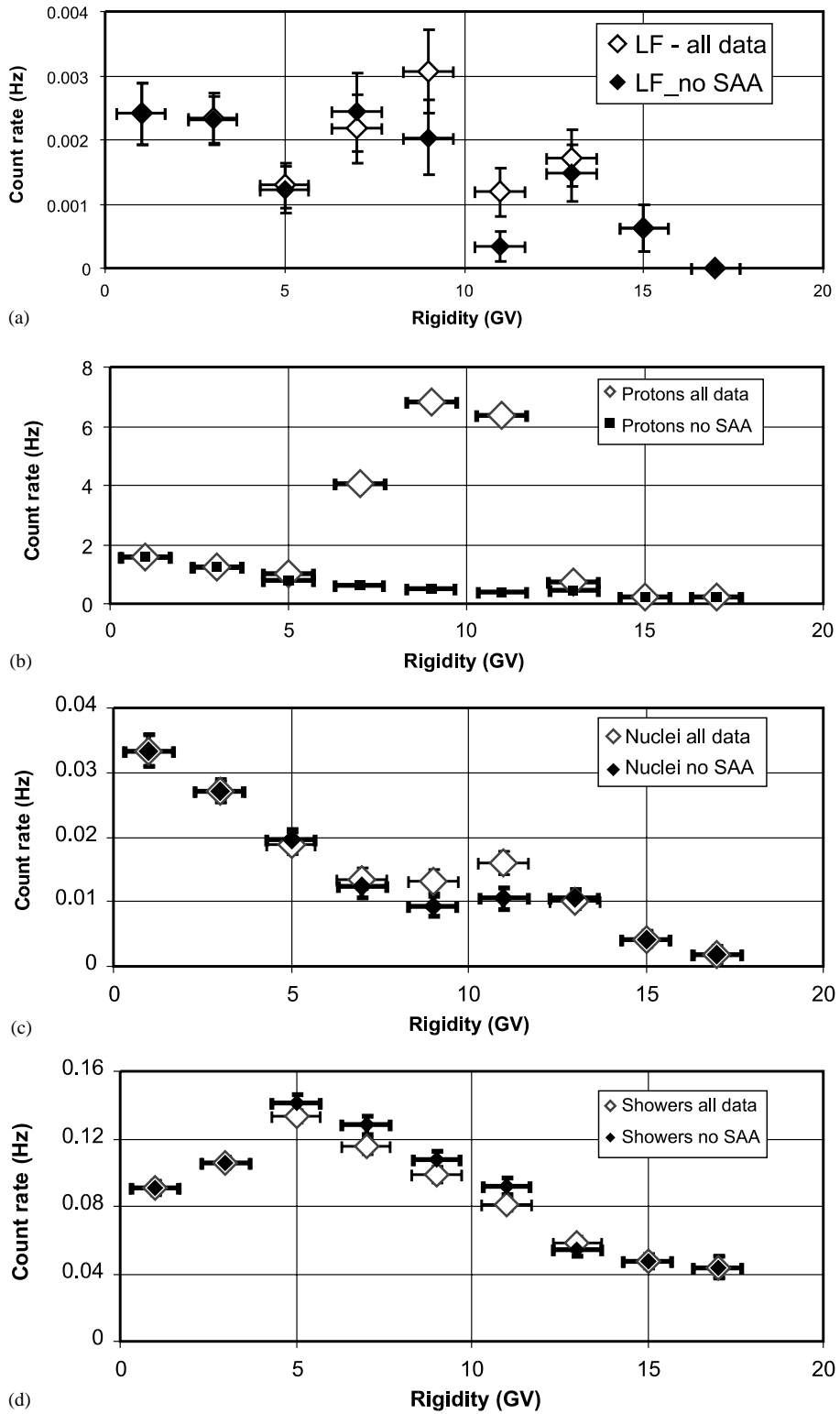


Fig. 9. Rates of LF (a), protons (b), nuclei (c) and showers (d) as functions of geomagnetic rigidity  $R$ . Open symbols show all data, filled symbols show data excluding SAA.

energy less than about 200 MeV, and in this range the proton rate is 22 times larger. The LF rate, on the other hand, is only two times larger in the SAA

than outside. We conclude that protons are not the main source of LFs, but we cannot exclude a contribution.

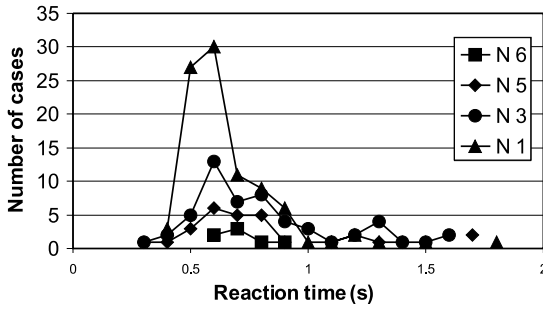


Fig. 10. Reaction time of four subjects to dark adaptation signals.

The strongest evidence for nuclei as the main source of LFs comes from comparing the proton and nucleus rates, between the “All time” column and the “In LF time window” column. The proton rate increases with about a factor of 2, while the nucleus rate is 6–7 times larger (Table 4).

We have eight very strong candidates of nuclei as initiators of LFs. These are from the tracks that

went through the eye in the LF time window. The charges of these eight candidates were estimated by the  $\sum E$  versus  $\Delta E$  scatter diagram (Fig. 5), as described in Section 3. Three particles have charge  $Z = 2$  (He), two are estimated to have  $Z = 2-3$  (He or Li), two candidates fall around  $Z = 8$  (O) and one is about  $Z = 24$  (Cr).

The probability that there is more than one nucleus in 1-s time interval is very small, since the overall rate of nuclei going through the eye is only about 1/100 s (see Table 4). So over the 116 LFs, we can expect one chance of simultaneous occurrence. Also showers that to a large fraction contain nuclei, will add to the probability of a chance correlation, and in about the same amount. Out of the eight strong candidates, two are therefore probably chance events.

If the source of LFs is mainly nuclei in our detector’s energy and charge range, and since the acceptance of the detector is only about 6–7%, from the 116 LFs observed, we would expect 7–8

Table 4. Events in LF time windows and tracks through an eye (all data)

Time-cut	All time (48 850 s)				In LF time window (total: 116 s)			
Eye-cut	All data		Track through eye		All data		Track through eye	
Event	Number	Rate (Hz)	Number	Rate (Hz)	Number	Rate (Hz)	Number	Rate (Hz)
Protons (p)	115,508	$2.50 \pm 0.01$	59 414	$1.29 \pm 0.005$	557	$5.1 \pm 0.2$	302	$2.8 \pm 0.2$
Nuclei (N)	858	$0.0186 \pm 0.0006$	479	$0.0104 \pm 0.0005$	11	$0.10 \pm 0.03$	8	$0.074 \pm 0.026$
Showers	4434	$0.0960 \pm 0.014$	—	—	10	$0.091 \pm 0.029$	—	—
LF	116	$0.0024 \pm 0.0002$	—	—	116	1	—	—
N/p		$0.0074 \pm 0.0002$		$0.0081 \pm 0.0004$		$0.020 \pm 0.006$		$0.026 \pm 0.009$
Showers/p		$0.0384 \pm 0.0006$		—		$0.018 \pm 0.006$		—

Table 5. Events in LF time windows and tracks through an eye (SAA data excluded)

Time-cut	All time (43 082 s)				In LF time window (total: 90 s)			
Eye-cut	All data		Track through eye		All data		Track through eye	
Event	Number	Rate (Hz)	Number	Rate (Hz)	Number	Rate (Hz)	Number	Rate (Hz)
Protons (p)	34,564	$0.822 \pm 0.004$	18 901	$0.450 \pm 0.003$	116	$1.3 \pm 0.1$	67	$0.76 \pm 0.09$
Nuclei (N)	756	$0.0180 \pm 0.0007$	428	$0.0102 \pm 0.0005$	10	$0.11 \pm 0.04$	7	$0.081 \pm 0.040$
Showers	4422	$0.105 \pm 0.002$	—	—	10	$0.11 \pm 0.04$	—	—
LF	90	$0.0021 \pm 0.0002$	—	—	90	1	—	—
N/p		$0.022 \pm 0.001$		$0.023 \pm 0.001$		$0.09 \pm 0.04$		$0.10 \pm 0.05$
Showers/p		$0.128 \pm 0.003$		—		$0.09 \pm 0.04$		—

Table 6. Events in LF time windows and tracks through an eye (only SAA data)

Time-cut	All time (9768 s)				In LF time window (total: 26 s)			
Eye-cut	All data		Track through eye		All data		Track through eye	
Event	Number	Rate (Hz)	Number	Rate (Hz)	Number	Rate (Hz)	Number	Rate (Hz)
Protons (p)	80,844	$17.80 \pm 0.06$	40 513	$8.92 \pm 0.04$	441	$21.5 \pm 1.0$	235	$11.5 \pm 0.7$
Nuclei (N)	102	$0.0225 \pm 0.0022$	51	$0.0112 \pm 0.0016$	1	$0.05 \pm 0.05$	1	$0.05 \pm 0.05$
Showers	12	$0.0026 \pm 0.0008$	—	—	—	—	—	—
LF	26	$0.0045 \pm 0.0009$	—	—	26	1	—	—
N/p		$0.0013 \pm 0.0001$		$0.0013 \pm 0.0002$		$0.002 \pm 0.002$		$0.004 \pm 0.004$
Showers/p		$0.00015 \pm 0.00004$		—		0		—

candidates. This is perfectly consistent with nuclei as the main source of LFs in space, but with some contribution from protons. The protons are likely to be of lower energy and therefore, more ionizing than high-energy protons.

#### 4.5. Particle - light flash probability

Assume that all LFs are caused by either nuclei or protons and that the detector efficiencies for these particle species are the same. Then, from the different rates in and out of SAA, we can calculate the probabilities for nuclei and protons, respectively, to cause an LF. Let  $R_p$  and  $R_N$  denote the event rates of protons and nuclei through the eyes outside SAA,  $R_{LF}$  the LF rate outside SAA, while  $S_p$ ,  $S_N$  and  $S_{LF}$  are the corresponding rates in the SAA. Further,  $\varepsilon_p$  and  $\varepsilon_N$  are the probabilities that a proton and a nucleus will cause an LF, respectively, while the detector-eye geometrical factor  $G$ , being the inverse of the acceptance, is about 6–7%. Then the following expressions are valid:

$$\begin{aligned} R_{LF} &= R_p G \varepsilon_p + R_N G \varepsilon_N, \\ S_{LF} &= S_p G \varepsilon_p + S_N G \varepsilon_N, \end{aligned} \quad (1)$$

from which one gets

$$\begin{aligned} \varepsilon_p &= \frac{S_N R_{LF} - R_N S_{LF}}{G(S_N R_p - S_p R_N)}, \\ \varepsilon_N &= \frac{S_p R_{LF} - R_p S_{LF}}{G(S_p R_N - S_N R_p)}, \end{aligned} \quad (2)$$

and in particular

$$\frac{\varepsilon_N}{\varepsilon_p} = \frac{S_p R_{LF} - R_p S_{LF}}{R_N S_{LF} - S_N R_{LF}}. \quad (3)$$

On inserting the numbers from Tables 5 and 6, one gets  $\varepsilon_N/\varepsilon_p = (7.5 \pm 3.5) \times 10^2$ . Taking  $G = 15$  ( $\approx 1/0.065$ ), the individual probabilities become  $\varepsilon_N = (1.3 \pm 0.2) \times 10^{-2}$  and  $\varepsilon_p = (1.7 \pm 0.8) \times 10^{-5}$ . As a consistency check, we can insert these values into the reverse formulae of expected number of light flashes ( $i = N$  or  $p$ ):

$$N_i = \varepsilon_i G (S_i t_{SAA} + R_i t_{noSAA}), \quad (4)$$

where  $t_{SAA}$  and  $t_{noSAA}$  are the observation times in SAA and outside, respectively. We then obtain 98 LFs from nuclei and 18 LFs from protons, adding up to 116, which is precisely the observed number. Thus, nuclei overwhelmingly dominate as initiators of LFs, which is consistent with what was found above.

Several error sources contribute to fairly large uncertainties in these numbers. The statistical error in  $\varepsilon_N$  is 13% while it is around 45% in  $\varepsilon_p$  and in

the ratio, dominated by  $S_{LF}(20\%)$ ,  $R_{LF}(11\%)$  and  $S_N(14\%)$ . The geometrical factor  $G$  is estimated with an error of about 25%, but it cancels in the ratio  $\varepsilon_N/\varepsilon_p$ . The probabilities are also an average over six different people, whereas some others did not see any, or very few LFs. There is a limited energy range of the detected particles; in particular, protons above 200 MeV are missing, and in general there might be different detector efficiencies for protons and nuclei. Actually, the ratio  $\varepsilon_N/\varepsilon_p$  is directly proportional to any correction due to differences in these detector efficiencies. Finally, any other source for LF is ignored.

Another possibility is that LFs caused by protons are from events with more than one proton hitting the eye at more or less the same time. The integration time of the eye,  $T_{eye}$ , is about 50 ms and during this time in the SAA, we get on an average  $0.050 G S_p = 6.7$  protons through the eyes. If the LF sensation is caused by a local effect in the retina, an added effect of several protons would require that the protons hit the same little area in the retina, which we call  $A_s$ . If we make the simplified assumption that outside SAA, all LFs are caused by nuclei, and the additional LF rate inside SAA is due to two protons hitting the same sensitive area within  $T_{eye}$ , we can get an estimate of the size of this area. Assuming all LFs outside SAA come from nuclei gives  $\varepsilon_N = 1.4 \times 10^{-2}$ , which is not much different from what we had above, but which would give a rate of LFs inside SAA from nuclei only of 0.0023 Hz. If the single hit rate in  $A_s$  is small ( $\ll 1$ ), one can approximate the double hit rate<sup>‡</sup> with

$$S_{2p} \approx (G S_p A_s / A_{eye})^2 T_{eye}, \quad (5)$$

where  $A_{eye}$  is the area of the whole eye. On introducing the “probability of a double proton hit to give an LF”,  $\varepsilon_{2p}$ , and with  $S_{2LF}$  being the LF rate in SAA due to double proton hits ( $0.0045 - 0.0023 = 0.0022$  Hz), one gets

$$\varepsilon_{2p} (A_s / A_{eye})^2 = S_{2LF} / (G^2 S_p^2 T_{eye}) = 2.5 \times 10^{-6}. \quad (6)$$

It is not reasonable that  $\varepsilon_{2p}$  would be larger than  $\varepsilon_N$ , which leads to  $A_s \geq 0.013 A_{eye}$ . However, even 1% of the area of the eye is likely to be too large “a single unit” in these circumstances. Even though the rate of all protons are much larger than the cut-off spectra of the SilEye detector measures, it seems

<sup>‡</sup>If the single rate is  $\rho$  and Poissonian, then the double hit rate in time windows  $T$  is given by  $\rho_2 = \rho(1 - e^{-\rho T})$ , which in case  $\rho T \ll 1$  is approximately equal to  $\rho^2 T$ .

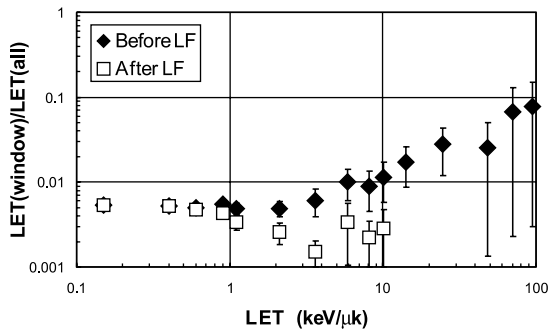


Fig. 11. Fraction of tracks through the eye, in LF-window ( $\blacklozenge$ ), and in “anti-LF” window ( $\square$ ), as a function of LET.

doubtful that double hits can give a significant contribution to LFs.

To conclude this part, it is estimated that about one nucleus in 100 passing through the eye would give rise to an LF, while only one proton in about 100,000 does the same.

#### 4.6. Linear energy transfer

We have studied the likelihood of a particle causing an LF as a function of its ionization, expressed in linear energy transfer (LET) in water as usually used in biological contexts. The LET for all tracks that passed through an eye was calculated. The fraction of tracks that occurred in the 116 LF-window (1.2–0.2 s before a registered LF signal, as used above) as a function of LET is shown in Fig. 11. For comparison, an “anti-LF” window was defined, being 0.2–1.2 s after the LFs. The corresponding fraction of tracks in the “anti-window” is also shown in Fig. 11. In the first sample (tracks falling in the LF-windows), we expect to find particles which could have made an LF, whereas no particle from the second sample (the “anti-windows”) could have caused an LF.

The fraction of tracks in the LF-window increases for LET-values larger than about 10 keV/ $\mu\text{m}$ , whereas the “anti-window” distribution is more or less flat. Actually, we do not find any particle with LET > 10 keV/ $\mu\text{m}$  in the “anti-window” distribution. The statistics is admittedly not large at high LET values, with only five events in the LF-window sample above 30 keV/ $\mu\text{m}$ , but it shows an increasing probability of creating LFs with increasing LET. This probability is about 5% at around 50 keV/ $\mu\text{m}$ . Not surprisingly, all the five highest LET events are found among the eight “strong candidates” for causing an LF, as described in Section 4.4.

## 5. CONCLUSIONS

Data on light flashes (LFs) in human eyes have been collected onboard the Russian space station Mir between 1995 and 1999 for the SilEye experiment. Six astronauts together spent over 26 h observing and noted 233 LFs during this time. Particle data, taken by the SilEye-2 detector and concurrent with the observations, have been used to correlate LFs with particles passing through the eyes.

Eight events with identified particles which most likely had caused an LF were found. Five of these were helium or lithium nuclei, two were oxygen nuclei and one was a heavy nucleus with charge  $Z$  around 24.

The rate of LFs inside the South Atlantic Anomaly (SAA) was found to be about twice as large as outside; however, the proton rate is many times higher inside than outside. On comparing rates of LFs, protons and nuclei inside and outside the SAA, we deduced that the probability of a nucleus passing through an eye to cause an LF is about 1%. The same probability for a proton with energy less than around 200 MeV, is roughly 750 times smaller than the nuclei probability. Higher energy protons are even less likely to make an LF.

As a function of ionization, expressed as linear energy transfer (LET) in water, there is a clear increase in probability that particles give rise to LFs for LET above 10 keV/ $\mu\text{m}$ , reaching about 5% at around 50 keV/ $\mu\text{m}$ .

The average observation time between LFs was 6.8 min, but this value depends on particle fluxes outside Mir — in particular inside or outside SAA, on different astronauts and possibly individuals’ sensitivity to LFs changes over time. No long-term space flight effect during one mission was found; however, there are indications that LF sensitivity decreases for subsequent flights, or with age. A possible effect of space adaptation, which would make people more sensitive to LFs during the first 1 or 2 weeks in space, could explain as to how during the Apollo program, it was consistently found that LF rates were much higher when going to the moon than when coming back. One SilEye subject made observations on his flight-days 5 and 8, and the results are consistent with this hypothesis, but certainly not conclusive. More flight data should be collected in the future.

The average LF rate during two observation sessions on Skylab in 1974 was about 10 times higher than what we found, and also during the Apollo–Soyuz test project in 1975, a significantly higher rate was measured. It is not clear as to where the widely different LF rates stem from, but it should be noted that the three space vehicles had different

material compositions and structures. No correlation with solar activity, as measured by the number of sun spots, was found.

About 90% of the LFs were described as appearing like a continuous line or a line with gaps. This is similar to results from Skylab, whereas from Apollo flights “spots” or “star-like” shapes were reported to dominate.

Dark adaptation and reaction time were measured at the start of each observation session, for control purposes. However, no difference was found for these physiological functions between ground and space, nor was any change over time in space noticed.

It has been shown that nuclei and largely ionizing particles are the dominant sources of light flashes in space (at least in a space station orbiting the Earth). From this, the Cherenkov effect can be excluded as one of the candidates for creating the light in the eye. Local energy deposition by ionization seems the most likely candidate. It still needs to be explained, though, as to how the energy gets transformed into a light signal to the brain. Is there any light involved, or is it perhaps direct stimulation of rods and cones by the penetrating particle? Other questions also remain, and particularly it is desirable to have measurements as independent as possible of subjective effects. Therefore, a continuation of the SilEye studies, under the name ALTEA, is planned for the International Space Station [25]. Among other features, ALTEA foresees the inclusion of EEG measurements simultaneous with LF observations and particle tracking detector data.

*Acknowledgements*—We would like to thank all astronauts who participated in the data collection onboard the Mir space station. ESA is acknowledged for providing a laptop for read-out and giving support. Financial support has been received from RFBR (Russian Foundation for Basic Research). The Swedish group thanks the Gustafsson foundation for support.

#### REFERENCES

1. Pinsky, L. S., et al., *Science*, 1974, **183**, 957; Osborne, W. Z., Pinsky, L. S., Baily, J. V., Apollo light flash investigations. Biomedical results of Apollo, NASA SP-386, 1975, p. 355.
2. Tobias, C. A., *Journal for Aviation Medicine*, 1952, **23**, 345.
3. Fremlin, J. H., *New Scientist*, 1970, **47**, 42.
4. Charman, W. H., Dennis, J. A., Fazio, G. G. and Jelley, J. V., *Nature*, 1971, **230**, 522.
5. Tobias, C. A., Budinger, T. F. and Lyman, J. T., *Nature*, 1971, **230**, 596.
6. Budinger, T. F., Bichsel, H. and Tobias, C. A., *Science*, 1971, **172**, 868.
7. Charman, W. N. and Rowlands, C. M., *Nature*, 1971, **232**, 574.
8. D’Arcy, F. J. and Porter, N. A., *Nature*, 1962, **196**, 1013.
9. McNulty, J., *Nature*, 1971, **234**, 110.
10. Akatov, Yu., et al., *Proceedings of the 6th European Symposium on Life Sciences Research in Space, Trondheim, Norway*, 1996, p. 153.
11. Fazio, G. G., Jelley, J. V. and Charman, W. N., *Nature*, 1970, **228**, 260.
12. McAulay, I. R., *Nature*, 1971, **232**, 421.
13. Budinger, T. F., Lyman, J. T. and Tobias, C. A., *Nature*, 1972, **239**, 209.
14. Budinger, T. F., et al., *Proceedings of the Colloquium Space Biology Related to Post-Apollo Programme, ESRO, Paris*, 1971, p. 235.
15. Pinsky, L. S., Osborne, W. Z., Hoffman, R. A. and Baily, J. V., *Science*, 1975, **188**, 928; Hoffman, R. A., Pinsky, L. S., Osborne, W. Z. and Baily, J. V., Visual light flash observation on Skylab 4, Biomedical results from Skylab, NASA SP-377, 1977, p. 127.
16. Budinger, T. F., et al., *Light flash observations. Experiment MA-106. Apollo-Soyuz Test Project Summary Science Report*, NASA SP-412, 1977, p. 193.
17. Bidoli, V., et al., *Nuclear Instruments and Methods A*, 1999, **424**, 414.
18. Bakaldin, A., et al., *Astroparticle Physics*, 1997, **8**, 109.
19. Casolino, M., et al., *Proceedings of the 26th ICRC, OG 4.2.17, Salt Lake City, USA*, 1999.
20. Adriani, O., et al., *Proceedings of the 26th ICRC, Vol. 5, OG 4.2.04, Salt Lake City, USA*, 1999, p. 96.
21. Bidoli, V., et al., *Nuclear Instruments and Methods A*, 1997, **399**, 477.
22. Furano, G., et al., *Proceedings of the 26th ICRC, Vol. 5, OG 4.2.13, Salt Lake City*, 1999, p. 128; Bidoli, V., et al., *Advances in Space Research*, 2000, **25**, 2075.
23. Galper, A. M., et al., *Proceedings of the 6th European Symposium on Life Sciences Research in Space, Trondheim, Norway*, 1996, p. 159.
24. Morselli, A., On behalf of the SilEye collaboration, *Proceedings of the 25th ICRC, Vol. 5, OG 10.2.8, Durban, South Africa*, 1997, p. 45.
25. Narici, L., et al., presented at the “Life Sciences in Space” Conference, May 2000, Santorini, Italy.